

Macrocyclic [N₅] transition metal complexes: synthesis, characterization and biological activities

Hanaa A. El-Boraey¹ · Mogda A. El-Salamony¹ · Abla A. Hathout¹

Received: 19 April 2016 / Accepted: 4 August 2016 / Published online: 18 August 2016
© Springer Science+Business Media Dordrecht 2016

Abstract Novel penta-azamacrocyclic 21-membered [N₅] ligand [L] and its transition metal complexes with Co(II), Ni(II), Cu(II), Ru(III) and Pd(II) have been isolated and characterized. The mode of bonding and overall geometry of the complexes have been inferred through IR, MS, UV–Vis, EPR, ¹H NMR spectral studies, molar conductivity, magnetic, thermal and microanalyses. On the basis of above studies, an octahedral geometry has been proposed for all complexes except Pd(II) chloride complex which adopt square planar geometry. The in vitro antitumor activity of the synthesized ligand and some selected complexes against human breast and human hepatocarcinoma cell lines (MCF-7) and (HePG2), respectively has been studied. The results show that the tested compounds are potent antitumor agents. Also the ligand and some selected complexes have been tested for their inhibitory effect on the growth of bacteria: *Streptococcus pyogenes* as Gram-positive bacteria and *Escherichia coli* as Gram-negative bacteria. The activity data show that most of the tested compounds exhibit remarkable antibacterial activity against these organisms.

Keywords Novel penta-azamacrocyclic · Macrocyclic metal complexes · Spectral studies · Biological activity

Electronic supplementary material The online version of this article (doi:10.1007/s10847-016-0649-5) contains supplementary material, which is available to authorized users.

✉ Hanaa A. El-Boraey
helboraey@yahoo.com

¹ Department of Chemistry, Faculty of Science, Menoufia University, Shebin El-Kom, Egypt

Introduction

Macrocycles and their metal complexes are of current interest due to their presence in many biologically significant systems [1–4]. Nitrogen-containing macrocycles have a strong tendency to form stable complexes with transition metals and have been reported to exhibit potent many biological activities [2, 5–9]. Polyaza macrocycles have attracted a considerable interest in recent years because of their ability to interact with both metal cationic and anionic species [10–15]. Among them, pentaazamacrocycles have been studied thoroughly; such ligands often lead to complexes with enhanced thermodynamic and kinetic stability with respect to metal ion dissociation, compared to their open-chain analogues. Much attention has been paid to macrocyclic compounds containing amide groups [16–21]. Due to the presence of proton donor (N–H) and proton acceptor (C=O), hydrogen bond formation is common in these macrocycles and affects their structure [12–19]. In the same aspect a large number of Schiff bases and their complexes have been studied for their interesting and important properties [22–28]. Recently, penta-aza and tetra-azamacrocycles and their transition metal complexes have been synthesized and characterized, their antitumor activity against human breast cancer cell line (MCF-7) and human hepatocarcinoma cell line (HePG2) has been studied [16, 29]. In the present study, we report the syntheses, spectroscopic characterization and thermal studies of novel Co(II), Ni(II), Cu(II), Ru(III), Pd(II) complexes with penta-azamacrocyclic ligand. These complexes have been characterized with the help of various physicochemical techniques. Furthermore, their in vitro antitumor activity against human breast (MCF-7) and human hepatocarcinoma cancer cell lines (HepG2) has been studied. Also the ligand and some selected complexes were screened against two

pathogenic bacteria *Streptococcus pyogenes* as Gram-positive bacteria and *Escherichia coli* as Gram-negative bacteria to assess their antibacterial activity.

Experimental

Materials

All reactions were carried out under normal atmospheric conditions. All the chemicals used in this study were of AnalaR grade and procured from Sigma, Aldrich and Fluka. Metal salts (E.Merck), i.e., $\text{Co}(\text{NO}_3)_2 \cdot 6\text{H}_2\text{O}$, $\text{Co}(\text{OAc})_2$, $\text{NiCl}_2 \cdot 6\text{H}_2\text{O}$, $\text{Ni}(\text{OAc})_2 \cdot 4\text{H}_2\text{O}$, $\text{CuCl}_2 \cdot 2\text{H}_2\text{O}$, $\text{Cu}(\text{NO}_3)_2 \cdot 3\text{H}_2\text{O}$, $\text{Cu}(\text{OAc})_2 \cdot 4\text{H}_2\text{O}$, CuBr_2 , $\text{RuCl}_3 \cdot 3\text{H}_2\text{O}$ and Na_2PdCl_4 and solvents were purchased commercially and used without further purification.

Isolation of the starting material

The starting material (S) has been synthesized as previously reported [29]. A mixture of 1H-benzo [d] [1,3] oxazine-2,4-dione (2.0 mmol, 2 g) with diethylenetriamine (1.0 mmol, 0.7 mL) in distilled water was stirred at 60 °C for about 3 h, heating on water bath was continued till the effervescence of CO_2 gas ceased. The reaction mixture was allowed to stand overnight. Dark brown precipitate obtained was filtered off and washed several times with cold distilled water. Recrystallization from ethanol gives compound: N,N'-(2,2-azanediylbis(ethane-2,1-diyl))bis(2-aminobenzamide) (S).

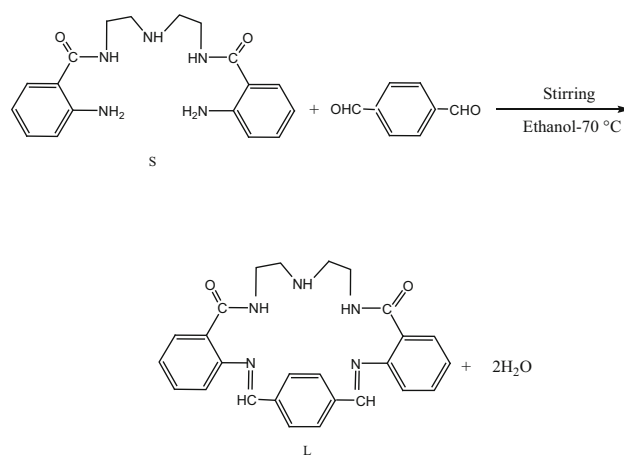
Color: dark brown, Yield: 50 %, m.p = 90 °C. Analysis Cal.(Found) for $\text{C}_{18}\text{H}_{23}\text{N}_5\text{O}_2 \cdot \text{H}_2\text{O}$ (MW:359) C,60.2(60.53); H,6.9 (6.8);N,19.5(18.8) % (KBr, cm^{-1}) 3340–3300 $\nu(\text{NH}/\text{NH}_2)$;1632 $\nu(\text{amide I})$;1525 [$\nu(\text{C-N}) + \delta(\text{N-H})$]; ^1H NMR (DMSO- d_6 , δ , ppm) $\delta = 6.48\text{--}7.49$ (8 H, ArH's), $\delta = 6.35$ (Ar-NH $_2$), $\delta = 3.8$ (NH amine), $\delta = 8.16\text{--}8.2$ (m, 2H, -NH-CO-), MS (EI+, m/z): Calc. for $\text{C}_{18}\text{H}_{23}\text{N}_5\text{O}_2$ (M = 341 Found: 340 [M-H] $^+$).

Isolation of the ligand

The starting material (1.0 mmol, 1 g) in acetone (20 mmol) was added to an ethanolic solution of terephthalaldehyde (1.0 mmol, 0.37 g), the resulting mixture was stirred at room temperature for about 2 h. The yellow solid precipitate was collected by filtration and washed several times with hot ethanol and dried over P_4O_{10} (m.p = 240 °C) (Scheme1).

Isolation of the macrocyclic complexes

All the macrocyclic metal complexes were prepared as follows:



Scheme 1 Preparation of the macrocyclic ligand

0.5 gm of the ligand was dissolved in 50 mL acetone, 20 mL ethanolic solution of different metal salt {chloride for complexes (3,5,9,10), nitrate for complexes (1,6), acetate for complexes (2,4,7) and bromide for complex (8)} was added dropwise in 1:1 (ligand: metal) molar ratio. For complex (4) the molar ratio was 1L: 2M. The reaction mixture was stirred under reflux whereupon the complexes precipitated. The precipitated solid complexes were separated from the solution by filtration, purified by washing several times with ethanol and then dried under vacuum at room temperature.

Physical measurements

The elemental analyses (C,H,N) were performed at Cairo University, Giza, Egypt using CHNS-932 (LECO) Vario Elemental Analyzer. Metals and halide analyses were estimated using standard methods.

The Fourier Transform Infrared (FTIR) measurements were performed (4000–400 cm^{-1}) in KBr discs using Nenexeus-Nicolidite-640-MSA FT-IR, Thermo-Electronics Co.

The UV–visible absorption spectra were measured in Nujol mull using 4802 UV/vis double beam spectrophotometer.

The ^1H NMR spectrum was recorded in DMSO- d_6 using Varian Gemini 200 NMR spectrophotometer at 300 MHz.

The EPR spectra were recorded using a Varian E-109C model X-band spectrometer. Molar conductivities were measured at 30 °C in DMSO solution (10^{-3} M) using a CON 6000 conductivity meter.

Magnetic susceptibilities of the complexes were measured at room temperature by the modified Gouy method using magnetic susceptibility Johnson Matthey Balance. The effective magnetic moments were calculated using the relation $\mu_{\text{eff}} = 2.828 (\chi_m T)^{1/2}$ B.M., where χ_m is the molar

susceptibility corrected for diamagnetism of all atoms in the compounds.

Thermal analysis (TG/DTG) was obtained out by using a Shimadzu DTA/TG-50 Thermal Analyzer with heating rate of 10 °C/min in nitrogen atmosphere with a following rate 20 mL/min in the range of ambient temperature up to 800 °C using platinum crucibles.

Electrospray mass spectra (ESI–MS) for the complexes were performed at the National Research Center, Egypt by the Thermo Electron Corporation. The electron impact (EI) mass spectrum for the ligand was run on Shimadzu-QP 2010 plus Mass Spectrometer, Microanalytical Laboratory, Faculty of Science, Cairo University, Egypt.

Biological tests

Anticancer activity

The in vitro anticancer activity of the compounds was tested at the National Cancer Institute, Cairo University Egypt by SRB assay using the method of Skehan et al. [30]. Two human tumor cell lines, liver (HepG2) and breast (MCF7) were used in the study and obtained from the American Type Culture Collection, Minnesota, USA. Cells were plated in 96-multiwell plate (10^4 cells/well) for 24 h before treatment with the compounds to allow attachment of cell to the wall of the plate. Different concentration of the compound under test (0, 2.5, 5, 10, 20 $\mu\text{g/mL}$) were added to the cell monolayer triplicate wells were prepared for each individual dose. Monolayer cells were incubated with the compounds for 48 h at 37 °C and in atmosphere of 5 % CO_2 . After 48 h, cells were fixed, washed and stained with Sulfo-Rhoda-mine-B stain. Excess stain was washed with acetic acid and attached stain was recovered with Tris EDTA buffer. Color intensity was measured in an ELISA reader. The relation between surviving fraction and drug concentration is plotted to get the survival curve of each tumor cell line after the specified compound.

Antibacterial activity

The in vitro antibacterial activity studies were carried out at Genetic Engineering and Biotechnology Research Institute, Department of Microbial Biotechnology at Sadat City University, Egypt, by using Broth Dilution Method [31] with some alterations, to investigate the inhibitory effect of the synthesized ligand and some complexes (**1,3–5,9**) on the sensitive organisms *Streptococcus pyogenes* as Gram-positive bacteria and *Escherichia coli* as Gram-negative bacteria. Nutrient broth medium was prepared by using Brain Heart Infusion (BHI) broth and distilled water. The test compounds in measured quantities were dissolved in DMSO which has no inhibition activity

to get two different concentrations (1 $\mu\text{g/mL}$, 5 $\mu\text{g/mL}$) of compounds. The strains selected for the study were prepared in (BHI) broth medium with shaking and autoclaved for 20 min 15 lb of pressure and at 121 °C before inoculation. The bacteria were then cultured for 24 h at 37 °C in an incubator. One ml of the standard bacterial culture was used as inoculation in a nutrient broth. For growth studies, culture of microbial cells were inoculated and grown aerobically in BHI broth for control and along with various concentrations of the test compounds in individual flasks. Growth was calculated turbidometrically at 650 nm using conventional Spectrophotometer, in which turbidity produced is measured by taking absorbance and compared with turbidity produced by control. The growth rate of different bacteria in absence as well as in presence of test compounds was performed for each concentration. Absorption measurements were accomplished by spectrophotometer after 24 and 48 h of incubation to determine the number of viable organisms per milliliter of sample and were used to the calculated the % inhibition.

Results and discussion

Physical properties

The condensation of the starting material (S) with terphthaldehyde affords 21-membered macrocyclic ligand (Scheme 1). Reaction of the resulting ligand with different transition metal salts affords the corresponding macrocyclic metal complexes. The microanalyses show that all complexes have 1L:1M stoichiometry except for complex (**4**) which shows 1L:2 M stoichiometry; the purity of the ligand and complexes has been checked by TLC. All the metals complexes are colored solids, stable towards air, slightly soluble in alcohols, insoluble in most common organic solvents, but soluble in DMF and/or DMSO. Crystals of these complexes could not be grown therefore X-ray crystal determination is not possible.

The molar conductance values in 10^{-3} M DMSO solution, measured at 30 °C, for the complexes were found to be low (Table 1). The relatively low values indicate the non-electrolytic nature of these complexes [32]. The relatively high value of conductance observed for complex (**3**) can be explained by the partial dissociation of the anion through the replacement by DMSO solution.

Mass spectrum of ligand

The electron impact (EI) mass spectrum of the free ligand (Fig. 1) showed a peak at 439 amu ($M + 1$) corresponding to the macrocyclic moiety ($\text{C}_{26}\text{H}_{25}\text{N}_5\text{O}_2$, atomic mass $m/z = 438$). The series of peaks in the range m/z

Table 1 Analytical and physical data for the ligand and its complexes

No.	Compound	Color	Empirical formula	Yield (%)	Decomp. Temp./°C	Elemental analysis Calc.(F) (%)				$(\Lambda_m)^a$
						C	H	N	M	
	L = $(C_{26}H_{25}N_5O_2) \cdot 1/2H_2O$	Brown	$C_{26}H_{28}N_5O_4(466)$	65	240 ^m	66.95 (66.14)	6.00 (5.92)	15.02 (15.10)	–	–
1	$[CoL(NO_3)(OH)] \cdot EtOH$	Brown	$C_{28}H_{32}N_6O_9Co$ M.W.(622.93)	80	210	53.93 (53.75)	5.13 (4.78)	13.48 (13.37)	9.46 (9.04)	7
2	$[Co(L)(OAc)_2] \cdot 4H_2O$	Brown	$C_{30}H_{39}N_5O_{10}Co$ (M.W.687.93)	70	220	52.33 (52.35)	5.66 (5.71)	10.17 (10.6)	8.53 (8.55)	2
3	$[Ni(L)Cl_2] \cdot 1/2EtOH$	Pale brown	$C_{27}H_{28}N_5O_{2.5}Cl_2Ni$ M.W.(591.71)	60	170	54.75 (54.61)	4.73 (4.92)	11.83 (11.04)	9.92 (10.00)	11.99 (11.90)
4	$[Ni_2(L)(OAc)_4(H_2O)_3] \cdot 4H_2O$	Dark yellow	$C_{34}H_{51}N_5O_{17}Ni_2$ M.W.(918.42)	70	220	44.42 (43.5)	5.55 (5.4)	7.61 (7.15)	12.78 (12.69)	–
5	$[Cu(L)Cl_2] \cdot EtOH \cdot H_2O$	Brown	$C_{28}H_{33}N_5O_4Cl_2Cu$ M.W.(637.54)	60	180	52.70 (52.36)	5.17 (5.00)	10.98 (11.10)	9.97 (10.35)	11.13 (11.5)
6	$[Cu(L)(NO_3)(OH)] \cdot 3H_2O$	Brown	$C_{26}H_{32}N_6O_9Cu$ M.W.(635.55)	76	220	49.09 (49.6)	5.03 (5.29)	13.21 (12.79)	9.99 (10.35)	–
7	$[Cu(L)(OAc)_2] \cdot 1/2EtOH$	Brown	$C_{31}H_{34}N_5O_{6.5}Cu$ M.W.(643.54)	70	150	57.8 (57.34)	5.28 (4.8)	10.8 (10.76)	9.87 (9.6)	–
8	$[Cu(L)(Br)_2] \cdot 3H_2O$	Dark grey	$C_{26}H_{31}N_5O_5Br_2Cu$ M.W.(716.34)	60	200	43.55 (43.5)	4.32 (3.90)	9.77 (9.00)	8.89 (9.6)	22.3 (22.0)
9	$[Ru(L)Cl_3(H_2O)] \cdot 2/2H_2O$	Black	$C_{26}H_{32}N_5O_{5.5}Cl_3Ru$ M.W.(709.1)	85	210	43.99 (43.9)	4.5 (4.54)	9.87 (9.61)	14.25 (14.14)	15.042 (15.7)
10	$[Pd(L)Cl_2] \cdot 1/2EtOH \cdot 2H_2O$	Black	$C_{26}H_{32}N_5O_{4.5}Cl_2Pd$ M.W.(675.40)	85	160	47.97 (48.56)	4.73 (4.7)	10.36 (9.92)	15.75 (16.00)	10.5 (11.8)

^a $\Omega^{-1} \text{ cm}^2 \text{ mol}^{-1}$ DMSO solutions (10^{-3} M)^b Partially soluble

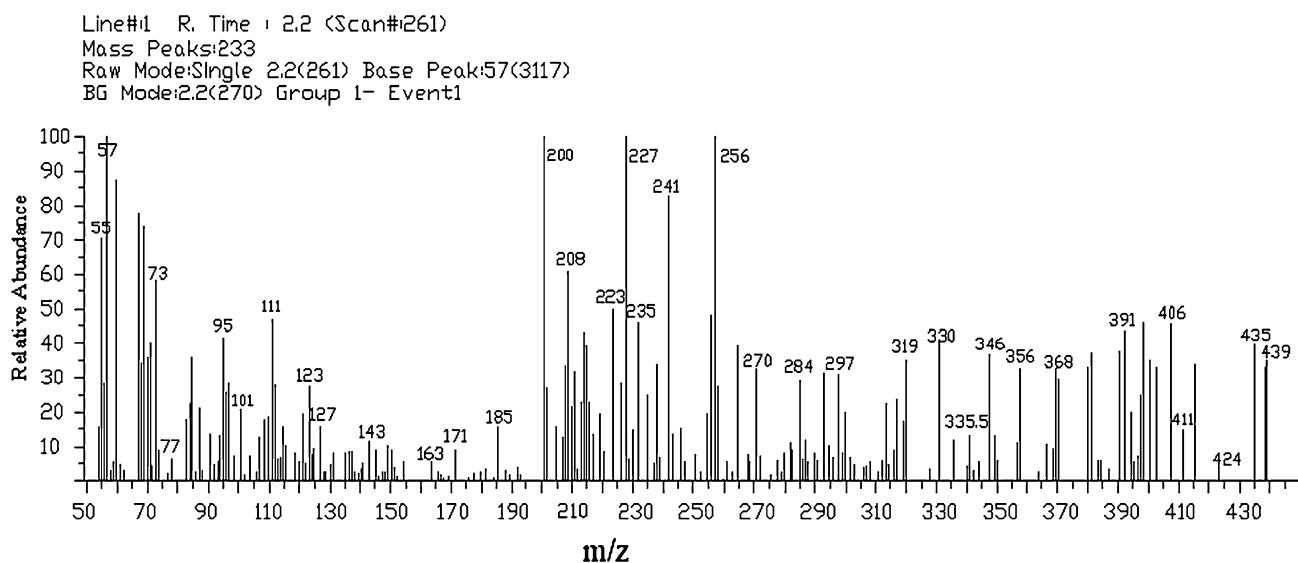


Fig. 1 The EI mass spectrum of ligand

$z = 76[\text{C}_6\text{H}_4]^+$, $102[\text{C}_8\text{H}_6]^+$, $234[\text{C}_{15}\text{H}_{10}\text{N}_2\text{O}]^+$, $335[\text{C}_{19}\text{H}_{20}\text{N}_5\text{O}]^+$, $411[\text{C}_{25}\text{H}_{25}\text{N}_5\text{O}]^+$, may be assigned to various fragments.

^1H NMR spectrum of the ligand

The ^1H NMR spectrum of the ligand was recorded in DMSO- d_6 solution. The spectrum shows that the different non-equivalent protons resonate at different values of applied field, signal at ca. δ 8.92 ppm (m, 2H, $-\text{CH}=\text{N}-$) is assigned to imine protons, signal at ca. δ 9.99 ppm (m, 2H, $-\text{NH}-\text{CO}-$) is assigned to amide proton, signal at δ (6.62–8.3 ppm) assigned to aromatic ring protons, signal at ca. δ 4.37 ppm assigned to $-\text{NH}$ of secondary amine protons and the multiple peaks observed in the region of $\text{NH}-\text{CH}_2$ and $\text{OC}-\text{NH}-\text{CH}_2$ signals indicate chemically nonequivalent methylene protons. Thus, the ^1H NMR result supports the assigned geometry.

IR spectra

Significant IR spectral bands of the macrocyclic ligand and its complexes are tabulated in Table 2. The IR spectrum of the free ligand is characterized mainly by the strong bands at 3192, 1634, 1617, 1508, 1291 and 752 cm^{-1} are attributed to the stretching frequencies of secondary amide/amine $\nu(\text{NH})$, amide-I [$\nu(\text{C}=\text{O})$], azomethine $\nu(\text{C}=\text{N})$, amide-II [$\nu(\text{C}-\text{N}) + \delta(\text{N}-\text{H})$], amide-III $\delta(\text{N}-\text{H})$ and amide-IV [$\varphi(\text{C}=\text{O})$] wagging vibrations, respectively, supporting the macrocyclic nature of the ligand [33, 34]. On complexation, the shift of $\nu(\text{C}=\text{N})$ frequency values in all complexes indicating the coordination of azomethine

nitrogen to the metal center [6, 26]. This is consistent with the presence of a new band at $490\text{--}400\text{ cm}^{-1}$ range assignable to $\nu(\text{M}-\text{N})$ vibration [19, 29]. The binding of secondary amide nitrogen in complexes is indicated by a shift of amide-I vibration from 1634 cm^{-1} in the free ligand to $1622\text{--}1612\text{ cm}^{-1}$ in the complexes [16]. The IR spectra of complexes (9,10) show that the band characteristic to amide I, $\nu(\text{C}=\text{O})$ appears nearly at the same position as that of the free ligand, indicating that this group does not participate in coordination. The appearance of new medium intensity band in the $625\text{--}530\text{ cm}^{-1}$ region, assigned to $\nu(\text{M}-\text{O})$. The broad band at $3478\text{--}3258\text{ cm}^{-1}$ is assigned to the stretching frequency $\nu(\text{OH})$ of solvent molecules, which is also confirmed from elemental and thermal analysis. Further, the complexes show the additional bands due to anions (Table 2). Complexes (1,6) show IR bands at $1383\text{--}1378$ (ν_5), $1297\text{--}1295$ (ν_1), $1047\text{--}1045$ (ν_2), $825\text{--}824$ (ν_3) cm^{-1} . The value of $\Delta(\nu_5 - \nu_1)$, i.e., $88\text{--}87\text{ cm}^{-1}$ suggesting the monodentate coordination of NO_3 ions [29]. Complexes (2,4,7) display bands at $(1580\text{--}1578)$ and $(1376\text{--}1375\text{ cm}^{-1})$, the difference of 204 cm^{-1} confirms the monodentate coordination of acetate ions [8, 19]. It is worth to mention that, the region of $\nu_{\text{asym}}(\text{COO}^-)$ overlapped with $\nu(\text{C}=\text{N})$ [35].

Mass spectrum of complex (3)

ESI-MS mass spectrum of the $[\text{Ni}(\text{L})\text{Cl}_2] \cdot \frac{1}{2}\text{EtOH}$, complex (3) was studied in DMSO solution (Fig. 2). The spectrum confirms the proposed formula by showing a molecular ion peak at m/z 590 amu corresponding to $[\text{Ni}(\text{L})\text{Cl}_2] \cdot \frac{1}{2}\text{EtOH}$ which coincide with its formula weight (calculated $m/z = 591.69$ amu). The other fragments of the

Table 2 Fundamental IR spectral bands (cm^{-1})^a of ligand and its metal complexes

No.	Compound	ν (OH/H ₂ O)	ν (NH)	ν (C=N)	Amide bands				ν (M–O)	ν (M–N)	Other assignments
					I	II	III	IV			
	L. 1/2H ₂ O	3751(b)	3192(b)	1617(b)	1634(sh)	1508(sh)	1291(m)	752(sh)	–	–	–
1	[Co(L)(NO ₃)(OH)]·EtOH	3333(b)	3291(b)	1618(b)	1618(b)	1508(m)	1266(b)	753(sh)	460(sh)	1383(b), 1295(sh), 1047(w), 825(w) (NO ₃ [–])	–
2	[Co(L)(OAc) ₂]·4H ₂ O	3478(b)	3335(b)	1580(b)	1612(m)	1515(b)	1242(w)	754(sh)	446(sh)	1580(b), 1376(w)(OAc) [–]	–
3	[Ni(L)Cl ₂]·1/2EtOH	3258(b)	3203(w)	1573(b)	1614(sh)	1500(w)	1281(sh)	656(sh)	480(w)	–	–
4	[Ni ₂ (L)(OAc) ₄ (H ₂ O) ₃]·4H ₂ O	3431(b)	3285(w)	1580(b)	1612(b)	1518(b)	1242(b)	681(sh)	400(w)	1580(b), 1376(w)(OAc) [–]	–
5	[Cu(L)Cl ₂]·EtOH·H ₂ O	3451(b)	3354(b)	1580(b)	1620(b)	1511(w)	1294(w)	759(m)	432(w)	–	–
6	[Cu(L)(NO ₃)(OH)]·3H ₂ O	3410(b)	3274(b)	1580(b)	1621(m)	1515(w)	1297(w)	760(m)	490(w)	1378.(sh), 1297(b), 1045(w),824(w) (NO ₃ [–])	–
7	[Cu(L)(OAc) ₂]·1/2EtOH	3412(b)	3259(w)	1578(b)	1622(b)	1518(m)	1261(w)	759(sh)	435(w)	–	–
8	[Cu(L)(Br) ₂]·3H ₂ O	3430(w)	3335(b)	1580(b)	1619(b)	1514(m)	1269(w)	760(sh)	443(w)	–	–
9	[Ru(L)Cl ₃ (H ₂ O)]·2/3H ₂ O	3396(b), 3343(m)	3202(b)	1605(b)	1634(sh)	1505(m)	1295(m)	766(m)	438(m)	–	–
10	[Pd(L)Cl ₂]·1/2EtOH·2H ₂ O	3429(b)	3300(b)	1611(b)	1634(sh)	1523(m)	1297(b)	754(sh)	458(w)	–	–

^a s strong, sh shoulder, m medium, w weak, b broad, v stretching^b Monodentate ion

complex give the peak with various intensities at different m/z values like at: Calc/Found 76/76 [C₆H₄]⁺, 102/103.93 [C₈H₆]⁺, 235/233 [M-(C₁₂H₁₈N₃O_{1.5} + NiCl₂)] + 3H⁺, 379.69/380.69[M-(C₁₂H₁₈N₂O_{1.5})⁺, 465.69/464.9[M-C₈H₇O_{1.5}]⁺, 540.69/544.2 [M-(1/2EtOH + CO), 568.69/570.22 [M-1/2EtOH]⁺.

¹H NMR spectrum of palladium(II) complex

¹H NMR spectrum of the [Pd(L)Cl₂]·1/2EtOH·2H₂O complex (**10**) was recorded in DMSO-*d*₆. ¹H NMR spectrum showed similar signals as for the ligand, but the position of the imine (–CH = N–) proton signal in the complex is shifted to 8.11 ppm in comparison with the free ligand (8.92 ppm), this observation supported the involvement of azomethine nitrogen in complex formation.

Magnetic susceptibility and electronic spectral studies

The electronic spectral measurements were used for assigning the stereochemistry of metal ions in the complexes based on the positions and number of d–d transition peak. The Nujol mull electronic absorption spectral data (λ_{max} , nm) of the complexes, room temperature effective magnetic moment values (B.M.) are tabulated (Table 3).

The electronic absorption spectra of Co(II) complexes (**1,2**) exhibit three bands at 660–640, 560–550 and 460 nm. The observed bands are assigned to the transitions ⁴T_{1g}(F) → ⁴T_{2g}(F)(ν_1); ⁴T_{1g}(F) → ⁴A_{2g}(F)(ν^2) and ⁴T_{1g}(F) → ⁴T_{2g}(P)(ν_3), respectively suggesting an octahedral geometry around Co(II) ion [36–38]. The magnetic susceptibility values are found to be 4.5, 5.4 B.M. (normal range for octahedral Co(II) complexes is 4.3–5.2 B.M.), which is an indicative of octahedral geometry [36].

The electronic absorption spectra of Ni(II) complexes (**3,4**) display three d–d transition bands at 680–660, 520–500 and 470 nm, attributable to the ³A_{2g} → ³T_{2g}(ν_1); ³A_{2g} → ³T_{1g}(ν_2); ³A_{2g} → ³T_{1g}(P)(ν_3) transitions, respectively in an octahedral symmetry [36, 38]. The magnetic moment values of Ni(II) complexes are found to be 3.0, 2.9 B.M., suggesting a high spin six-coordinated octahedral [38] arrangement of ligand molecules around the metal ion.

The electronic spectra of Cu(II) complexes (**5–8**) exhibit bands in the region 720–680, 540–530 and 480–460 nm, are assigned to ²B_{1g} → ²A_{1g} (ν_1); ²B_{1g} → ²B_{2g} (ν_2) and ²B_{1g} → ²E_g (ν_3) transitions, respectively. Which showed that these complexes are tetragonally distorted [1, 20]. The magnetic moment values for Cu(II) complexes lie in the 1.8–1.9 B.M. range corresponding to one unpaired electron [36].

Electronic absorption spectrum of Ru(III) complex (**9**) exhibits moderately intense band in the visible region at

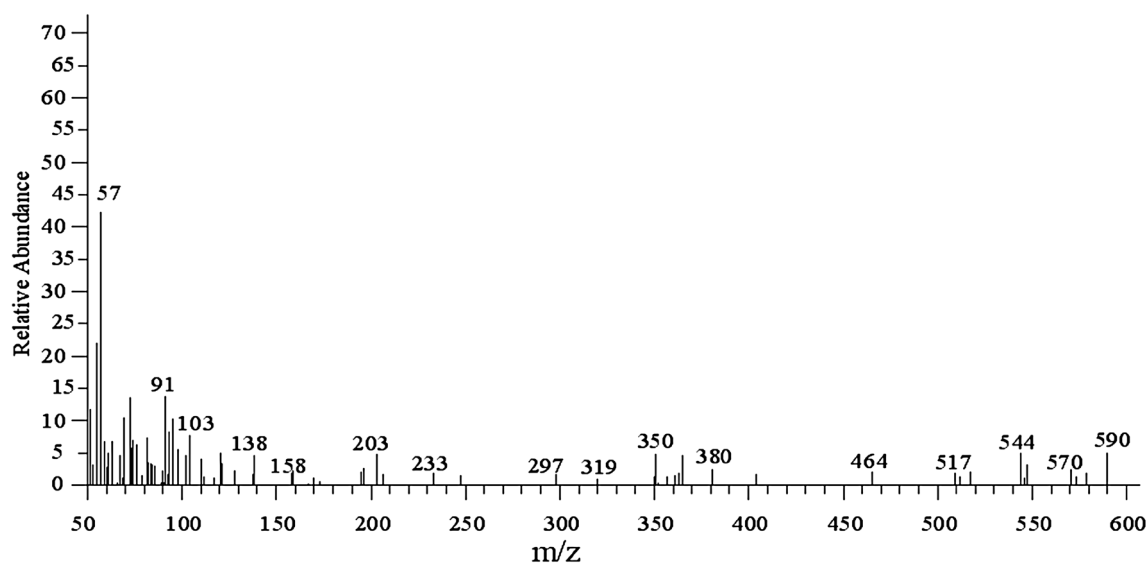


Fig. 2 The ESI mass spectrum of $[\text{Ni}(\text{L})\text{Cl}_2] \cdot \frac{1}{2}\text{EtOH}(\mathbf{3})$

Table 3 Electronic absorption spectra (λ_{max} , nm), effective magnetic moment values (μ_{eff} , B.M.) of complexes

No.	Complexes	λ_{max} (Nujol mull, nm)		μ_{eff} (B.M./ M^{+n})
		(d–d) transition	Intraligand and charge transfer bands	
	Ligand. $\frac{1}{2}\text{H}_2\text{O}$	–	–450, 320, 260	–
1	$[\text{CoL}(\text{NO}_3)(\text{OH})] \cdot \text{EtOH}$	640, 550, 460	380, 280	4.5
2	$[\text{Co}(\text{L})(\text{OAc})_2] \cdot 4\text{H}_2\text{O}$	660, 560, 460	350, 280	5.4
3	$[\text{Ni}(\text{L})\text{Cl}_2] \cdot \frac{1}{2}\text{EtOH}$	680, 500, 470	267, 260	3.0
4	$[\text{Ni}_2(\text{L})(\text{OAc})_4(\text{H}_2\text{O})_3] \cdot 4\text{H}_2\text{O}$	660, 520, 470	350, 280	2.9
5	$[\text{Cu}(\text{L})\text{Cl}_2] \cdot \text{EtOH} \cdot \text{H}_2\text{O}$	720, 530, 460	350, 260	1.8
6	$[\text{Cu}(\text{L})(\text{NO}_3)(\text{OH})] \cdot 3\text{H}_2\text{O}$	690, 540, 480	340, 280	1.99
7	$[\text{Cu}(\text{L})(\text{OAc})_2] \cdot \frac{1}{2}\text{EtOH}$	680, 540, 480	340, 260	1.9
8	$[\text{Cu}(\text{L})(\text{Br})_2] \cdot 3\text{H}_2\text{O}$	680, 550, 460	380, 280	1.85
9	$[\text{Ru}(\text{L})\text{Cl}_3(\text{H}_2\text{O})] \cdot 2\frac{1}{2}\text{H}_2\text{O}$	640, 500	270	2.5
10	$[\text{Pd}(\text{L})\text{Cl}_2] \cdot \frac{1}{2}\text{EtOH} \cdot 2\text{H}_2\text{O}$	640, 520, 430	350, 270	(Dia) ^a

^a Diamagnetic

640 nm due to d–d transition and an absorption band at 500 nm probably due to MLCT transition [16, 39]. Its magnetic moment at room temperature is 2.5 B.M., corresponding to one unpaired electron. Electronic absorption spectrum of Pd(II) complex (**10**) shows three bands at 640, 520, 430 nm assignable to $^1\text{A}_{1g} \rightarrow ^1\text{A}_{2g}$, $^1\text{A}_{1g} \rightarrow ^1\text{B}_{1g}$ and $^1\text{A}_{1g} \rightarrow ^1\text{E}_g$ transitions, respectively [20, 40]. Diamagnetic behavior and molar conductance value (Table 1) confirming the square planar geometry of this complex [40].

ESR studies

ESR spectra of the copper(II) complexes (**6–8**) were recorded in solid state at room temperature on the X-band frequency

9.771 GHz. The ESR parameters are tabulated (Table 4). All complexes give axially symmetric g -tensor parameters with g_{\parallel} (2.17–2.28) > g_{\perp} (2.043–2.06) > 2.0023 indicating that the copper site has a $d_{x^2-y^2}$ ground state, characteristic of an octahedral stereochemistry [41, 42]. Also the observed

Table 4 EPR parameters for the Cu(II) complexes as polycrystalline sample at RT

No.	Compound	g_{\parallel}	g_{\perp}	g_{av}	G
6	$[\text{Cu}(\text{L})(\text{NO}_3)(\text{OH})] \cdot 3\text{H}_2\text{O}$	2.28	2.059	2.136	4.74
7	$[\text{Cu}(\text{L})(\text{OAc})_2] \cdot \frac{1}{2}\text{EtOH}$	2.17	2.042	2.085	4.2
8	$[\text{Cu}(\text{L})(\text{Br})_2] \cdot 3\text{H}_2\text{O}$	2.25	2.065	2.129	4.06

$g_{//}$ values are less than 2.3 provide evidence for appreciable covalent character for Cu–L bond [43]. The geometric parameter G , which is a measure of exchange interaction between the copper centers in the polycrystalline compounds, is calculated by using the expression: $G = g_{//} - 2.0023/g_{\perp} - 2.0023$.

According to Hathaway [44] as value of G is greater than 4, the exchange interaction between copper(II) centers in the solid state is negligible, whereas when it is less than 4, a considerable exchange interaction is indicated in the solid complex. For copper(II) complexes (6–8), the calculated G value is higher than 4 (Table 4) indicating that the interaction between metal centers is negligible [45].

Thermal studies

Thermal behavior of the ligand and its complexes has been studied using TG/DTG measurements. The TGA/DTG curves of macrocyclic ligand and its complexes were recorded in nitrogen atmosphere from room temperature up to 800 °C; important data are listed in Table 1S. The results obtained from thermogravimetric analysis were in agreement with the suggested theoretical formula from the elemental analysis.

For the macrocyclic ligand, the TG curve shows weight loss of 5.73 % (Calc 5.79 %); in the temperature range of 30–144 °C. The endothermic DTG peak recorded at 43 °C reflect the loss of one and half water molecules per ligand molecule. Also the TG curve shows two decomposition steps in the temperature range 240–760 °C with total weight loss of 100 %. These results agree well with the composition of the ligand determined from elemental analysis and IR spectrum.

The TG curves of cobalt(II) complexes (1,2) shows weight loss in the temperature range 30–130 °C (Calc/Found % 7.96/8.16; 10.4/9.8), respectively associated with endothermic DTG peak at 72.52 °C, that are assigned to release of one ethanol molecule (complex 1) and four water molecules (complex 2). The TG curves also show that the complexes gradually decomposed at 215 and 220 °C ended with the formation of Co for complex 1 and CoO for complex 2, respectively.

The TG curves of nickel(II) complexes (3,4) show weight loss in the temperature range 30–145 °C (Calc/Found % 3.8/3.82, 7.8/7.17), respectively associated with two endothermic DTG peak at 51 and at 50 °C, that are assigned to release of half ethanol molecule (complex 3) and four water molecules (complex 4, Fig. 3). The TG

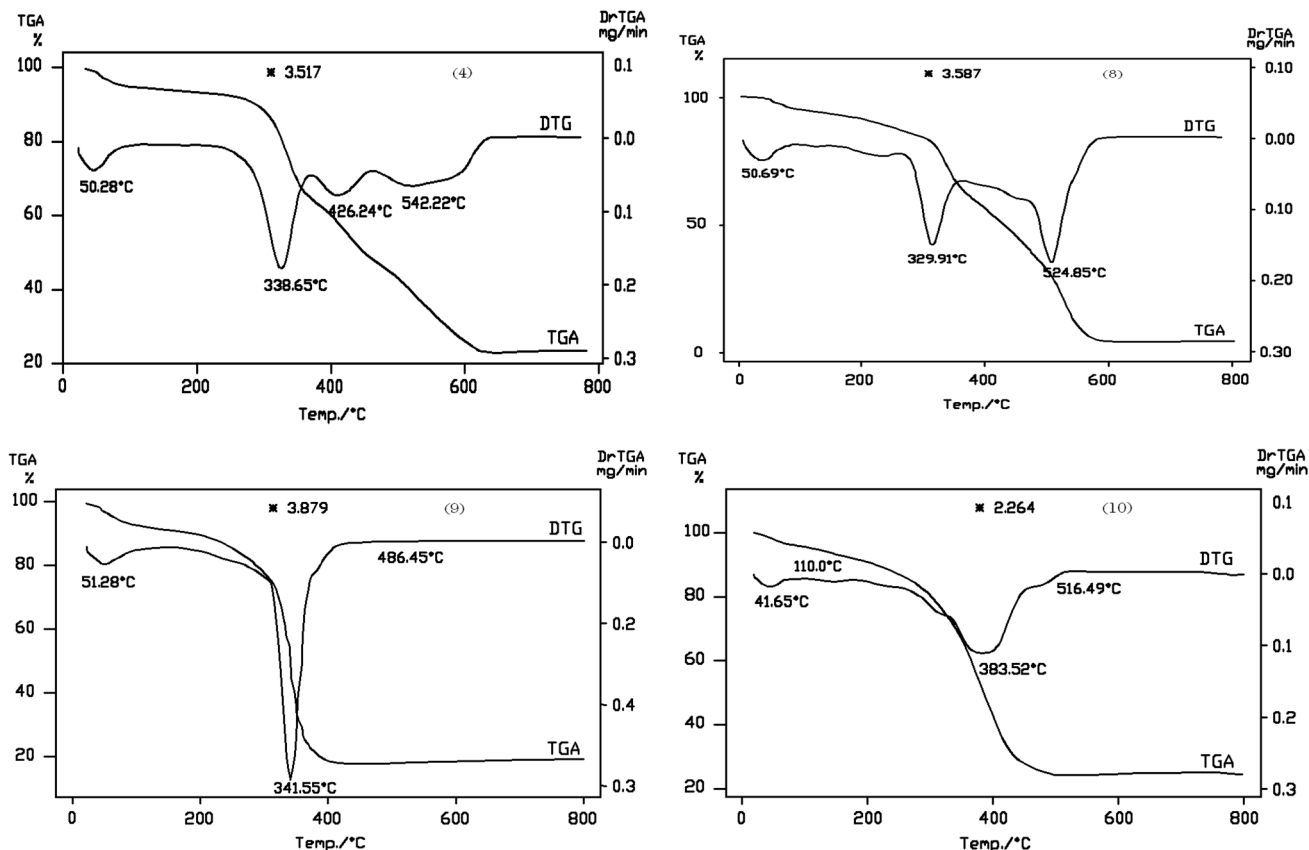


Fig. 3 TG/DTA curves of complexes (4, 8, 9, 10). *Mass of sample (mg)

curves also show that the complexes gradually decomposed at 170 and 220 °C ended with the formation of NiO for both complexes.

The TG curves of copper complexes (5–8) show weight loss in the temperature range 30–175 °C (Calc/Found % 10,0/10.1;8.4/8.4;7.5/7.6;3.5/3.5), respectively associated with endothermic DTG peak at 59 °C, that is assigned to release ethanol and water molecules in two steps (complex 5), peak at 59 °C, that is assigned to release of three water molecules (complex 6), peak at 47 °C, that is assigned to release of half ethanol molecule (complex 7), peak at 50 °C, that is assigned to release of three water molecules (complex 8, Fig. 3). The TG curves also show that the complexes gradually decomposed in more than one stage, ended with the formation of CuO for all complexes (Table 1S).

The TG curve of ruthenium(III) complex (9) shows weight loss in the temperature range 30–115 °C (Calc/Found % 6.35/6.16) associated with a broad DTG peak at 51 °C, that is assigned to release of two and half water molecules (Fig. 3). The TG curve also shows that the complex starts decomposition at 210 °C, ended with the formation of RuO₂ as final decomposition product.

The TG curves of palladium(II) complex (10) shows weight loss in the temperature range 30–125 °C (Calc/Found % 8.74/8.06) associated with endothermic DTG peak at 42 °C, that is assigned to release of half ethanol and two water molecules in two steps (Fig. 3). The TG curve also shows that the complex starts decomposition at 160 °C given PdO as final decomposition product. It is worth to note that, The slight higher value found for the percentage of the residue when compared with the theoretical value for pure metal oxide in complexes (2,4,10) shows that the residue is contaminated with carbon [46–48]. The nature of the remaining residues was reported and identified by IR spectroscopy.

Kinetic and thermodynamic parameters

The kinetic and thermodynamic parameters of the decomposition stages of the desolvated complexes (1–10) were determined from TG curve using the Coats–Redfern equation [49]. The Horowitz and Metzger [50] equation $C_s = (n)^{1/1-n}$ was used for the determination of the value of the reaction order, and given by:

$$C_s = \frac{m_s - m_\infty}{m_0 - m_\infty}$$

where C_s is the weight fraction of the substance present at DTG peak temperature T_s , m_s is the remaining weight at T_s , m_0 and m_∞ are the initial and final weights of the substance, respectively. The estimated values of C_s for the thermal decomposition of the desolvated complexes were found in the range of 0.25–0.393 (Table 5). This indicated that the decomposition follows first order kinetic [16, 29]. So, the values of the activation energy E^* , Arrhenius constant A , the activation entropy S^* , the activation enthalpy H^* and the Gibbs free energy of activation G^* are calculated by applying Coats–Redfern equation for $n = 1$

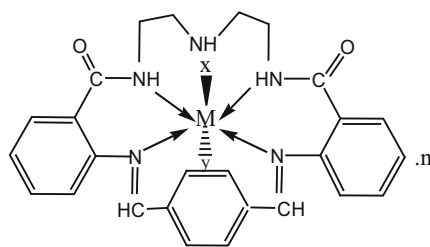
$$\log \left[\frac{-\log(1-x)}{T^2} \right] = \log \frac{AR}{\theta E^*} \left(1 - \frac{2RT}{\Delta E^*} \right) - \frac{\Delta E^*}{2.303RT} \quad (1)$$

where x is the fraction decomposed, R : is the gas constant and θ is the heating rate. Since $(1 - 2RT/E^*) \simeq 1$, a plot of the left-hand side of Eq. (1) against $1/T$ gives a straight line from its slope and intercept, E^* and A were calculated (Table 5). The entropy of activation S^* , enthalpy of activation H^* and the free energy change of activation G^* were calculated using the following equations [51].

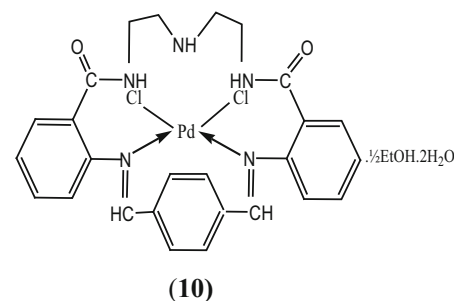
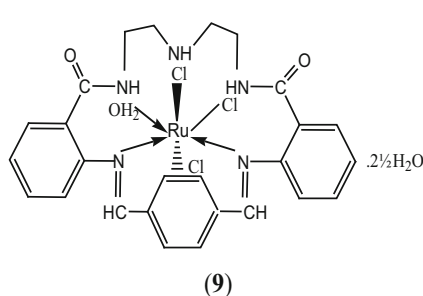
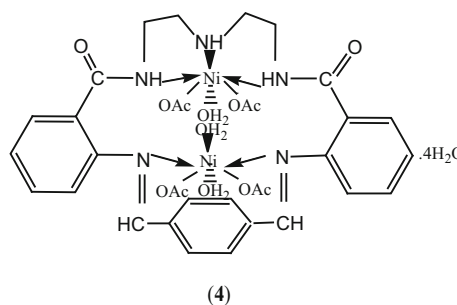
$$\Delta S^* = [\ln(Ah/kT) - 1]R, \quad \Delta H^* = \Delta E^* - RT, \\ \Delta G^* = \Delta H^* - T\Delta S^*.$$

Table 5 Kinetic and thermodynamic data of the complexes

No.	Complex	Decomp. temp./ (K)	A (S^{-1})	ΔS^* ($J \text{ mol}^{-1} K^{-1}$)	ΔE^* ($kJ \text{ mol}^{-1}$)	ΔH^*	ΔG^*	C_s
1	[Co(L)(NO ₃)(OH)]·EtOH	493–923	15.16 E ⁹	−8.95	37.24	30.9417	37.71	0.356
2	[Co(L)(OAc) ₂]·4H ₂ O	488–902	19.50 E ⁹	−16.23	28.20	23.43	32.74	0.333
3	[Ni(L)Cl ₂]·½EtOH	508–658	6.87 E ⁹	−7.105	25.54	22.22	25.05	0.393
4	[Ni ₂ (L)(OAc) ₄ (H ₂ O) ₃]·4H ₂ O	493–929	4.166 E ⁸	−10.12	43.64	39.529	44.518	0.351
5	[Cu(L)Cl ₂]·EtOH·H ₂ O	508–658	7.28 E ⁹	−7.20	42.88	38.99	46.20	0.33
6	[Cu(L)(NO ₃)(OH)]·3H ₂ O	494–726	11.54 E ⁹	−6.88	19.16	14.69	11.00	0.34
7	[Cu(L)(OAc) ₂]·½EtOH	493–708	15.56 E ⁸	−6.196	37.36	34.33	37.61	0.351
8	[Cu(L)Br ₂]·3H ₂ O	538–665	2.798 E ¹¹	−3.837	146.88	14.69	11.00	0.32
9	[Ru(L)Cl ₃ (H ₂ O)]·2½H ₂ O	398–697	6.860 E ⁷	−12.143	45.33	40.25	47.68	0.293
10	[Pd(L)Cl ₂]·½EtOH·2H ₂ O	398–768	13.233 E ⁸	−9.293	37.28	42.95	49.29	0.25

Scheme 2 Suggested structure of the complexes

No.	M	x	y	n
(1)	Co(II)	NO ₃	OH	EtOH
(2)	Co(II)	OAc	OAc	4H ₂ O
(3)	Ni(II)	Cl	Cl	½EtOH
(5)	Cu(II)	Cl	Cl	EtOH.H ₂ O
(6)	Cu(II)	NO ₃	OH	3H ₂ O
(7)	Cu(II)	OAc	OAc	½EtOH
(8)	Cu(II)	Br	Br	3H ₂ O



The calculated kinetic and thermodynamic values are listed in Table 5.

The high ΔE^* values reveal high stability of the chelates and the positive values of ΔH^* indicating endothermic process. The Gibbs free energy of activation ΔG^* is used to determine the spontaneity of the chemical reactions. Table 5 shows that all complexes presented positive value of ΔG^* indicating that they are endergonic and not spontaneous. Negative ΔS^* values may arise as a result of association mechanism; degrees of freedom were lost due to the activated complex formation, which means that reacting species joined themselves to form the state transition during the reaction, thereby having a more ordered state than the reactants in the ground state structure [52]. The correlation coefficients of the

Arrhenius plots of the thermal decomposition steps were found to lie in the range 0.9887–0.9777 showing a good fit with linear function.

From interpretation of the elemental analyses, infrared, electronic, ESR, mass, ¹H NMR spectra, magnetic susceptibility, thermal and molar conductivity it is possible to draw up the tentative structures of the metal complexes, Scheme 2.

Biological activity

Anticancer activity

Transitional metal chemistry is evolving for its capacity to target biological molecules. There exists considerable

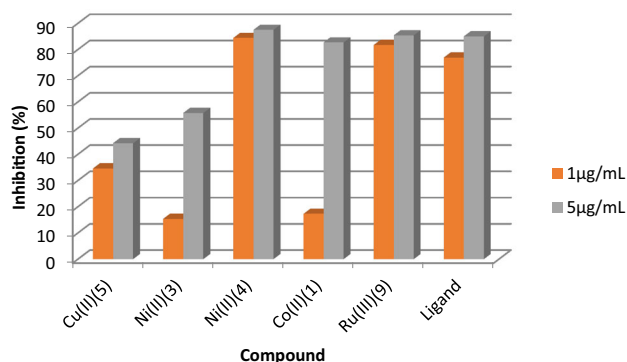


Fig. 4 In vitro antibacterial activity of the complexes and metal free macrocycle ligand against *S. pyogenes*

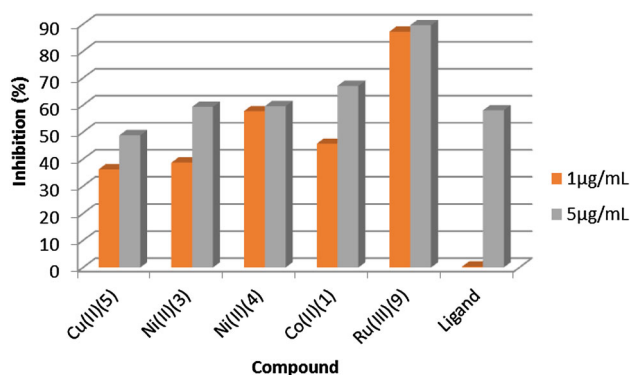


Fig. 5 In vitro antibacterial activity of the complexes and metal free macrocycle ligand against *E. coli*

interest for the discovery of new metal based anticancer drugs. Here we have checked the anticancer activities of the macrocyclic ligand and some of its complexes. The results of the cytotoxic activity in vitro were expressed as IC_{50} (the concentration of the compound in $\mu\text{g/mL}$ that inhibits proliferation of the cells by 50 % as compared to the untreated control cells) are given in Table 6. The ligand shows IC_{50} value of 3.0 and 3.3 $\mu\text{g/mL}$ toward human breast cancer cell line (MCF-7) and human hepatocarcinoma cells (HepG2), respectively and that for some selected complexes (3,5,9,10) were in the range of 2.0–8.3 $\mu\text{g/mL}$ toward the former cell and 2.2–8.5 $\mu\text{g/mL}$ toward the latter one, respectively. Shier [53] suggested that compounds exhibiting IC_{50} values more than 10–25 $\mu\text{g/mL}$ indicate weak cytotoxic activities while compounds with IC_{50} values less than 5 $\mu\text{g/mL}$ are considered to be very active. Those having intermediate values ranging from 5 to 10 $\mu\text{g/mL}$ are classified as moderately active. Accordingly, the ligand and its complexes (3,9) ($IC_{50} = 2.0$ – $2.6 \mu\text{g/mL}$) are considered to be very active toward both human breast cancer and hepatocarcinoma cells. Whereas complexes (5), (10) are classified as moderately active on human breast and human hepatocarcinoma cancer cell lines, IC_{50} value = 5.6–8.3 $\mu\text{g/mL}$.

Table 6 Lethal concentration (IC_{50}) of the ligand and its metal complexes on MCF-7 and HepG2

No.	Compound	IC_{50} ($\mu\text{g/mL}$) ^a	
		MCF-7	HepG2
	L. $1\frac{1}{2}\text{H}_2\text{O}$	3.0	3.30
3	$[\text{Ni}(\text{L})\text{Cl}_2] \cdot 1\frac{1}{2}\text{EtOH}$	2.0	2.20
5	$[\text{Cu}(\text{L})\text{Cl}_2] \cdot \frac{1}{2}\text{EtOH} \cdot \text{H}_2\text{O}$	5.60	6.00
9	$[\text{Ru}(\text{L})\text{Cl}_3(\text{H}_2\text{O})] \cdot 2\frac{1}{2}\text{H}_2\text{O}$	2.30	2.60
10	$[\text{Pd}(\text{L})\text{Cl}_2] \cdot \frac{1}{2}\text{EtOH} \cdot 2\text{H}_2\text{O}$	8.30	8.50

^a (IC_{50}) is the concentration of compound ($\mu\text{g/mL}$) that inhibits a proliferation rate of the tumor cells by 50 % as compared to control untreated cells

The results also show that Ni(II) complex (3) showed highest cytotoxic activity on both human breast and human hepatocarcinoma cancer cell lines, IC_{50} value = 2.0, 2.2 $\mu\text{g/mL}$. The enhanced activity of the tested compounds were consistent with and better than the documented activity of similar compounds as antitumor agents [54–58]. The/enhanced activity may be attributed to the increase in conjugation in the ligand moiety on complexation [59]. The type of metal ions may be another reason for their different anticancer activity. The active sequence of the ligand and its complexes follows the trend:

Ni(II) > Ru(III) > L > Cu(II) > Pd(II) for MCF-7 cells,
Ni(II) > Ru(III) > L > Cu(II) > Pd(II) for HepG2 cells.

Antibacterial activity

The synthesized ligand and its metal complexes [Co(II)(1), Ni(II)(3), (4), Cu(II) (5) and Ru(III) (9)] were screened for antibacterial activity against the tested pathogens, according to the data depicted in Figs. 4 and 5 and tabulated in Table 7. The following results are obtained:

The tested compounds are found to have remarkable biological activity. The antibacterial activity of the tested compounds in the concentration 1 $\mu\text{g/mL}$ is found to follow the order; Ni(II)(4) > Ru(III)(9) > L > Cu(II)(5) > Co(II)(1) > Ni(II)(3) for the concentration 5 $\mu\text{g/mL}$ the order is: Ni(II)(4) > Ru(III)(9) \geq L \geq Co(II)(1) > Ni(II)(3) > Cu(II) (5) for Gram- positive. With regard to Gram-negative bacteria the order is: Ru(III) (9) > Ni(II)(4) > Co(II) (1) > Ni(II)(3) > Cu(II) (5) > L for concentration 1 $\mu\text{g/mL}$ and Ru(III) (9) > Co(II) (1) > Ni(II)(4) \geq Ni(II) (3) \geq L > Cu(II) (5) for the concentration 5 $\mu\text{g/mL}$.

It is found that Ni(II)(4) and Ru(III) (9) complexes have higher antibacterial activity against both Gram-positive and Gram-negative bacteria than the free macrocyclic ligand for both concentrations. Also, it is found that all complexes except Cu(II)(5) complex (5 $\mu\text{g/mL}$) have higher

Table 7 Inhibition (%) of the ligand and its metal complexes against *S.pyogenes* and *E.coli* bacteria

No.	Compound	Inhibition (%)			
		<i>S.pyogenes</i>		<i>E.coli</i>	
		1 µg/mL	5 µg/mL	1 µg/mL	1 µg/mL
	L. 1½H ₂ O	76.92	85	0.39	58.026
1	[Co(L)(NO ₃)(OH)]·EtOH	17.3	82.69	45.66	67.11
3	[Ni(L)Cl ₂]·½EtOH	15.38	55.769	38.68	59.34
4	[Ni ₂ (L)(OAc) ₄ (H ₂ O) ₃]·4H ₂ O	84.42	87.5	57.24	59.61
5	[Cu (L)Cl ₂]·½EtOH.H ₂ O	34.6	44.25	36.18	48.82
9	[Ru(L)Cl ₃](H ₂ O)]·2½H ₂ O	81.73	85.38	87.24	89.61

antibacterial activity against Gram negative bacteria than the free macrocycle ligand.

This would suggest that the chelation could facilitate the ability of a complex to cross a cell membrane and can be explained by Tweedy's chelation theory [60]. Chelation/complexation could enhance the lipophilic nature of the central metal atom, which subsequently favors its permeation through the lipid layer of the cell membrane. In addition, other factors such as solubility, dipole moment, conductivity influenced by metal ion may be possible reasons for remarkable antibacterial activities of these complexes. It also has been observed that some moieties such as azomethine linkage introduced into such compounds exhibits extensive biological activity [61, 62].

Conclusions

In this study a novel pentaaza (N₅) macrocyclic ligand and its corresponding transition metal complexes (**1–10**) have been synthesized and characterized. Based on various physicochemical studies as elemental analyses, conductivity, magnetic, spectral (electronic, EPR, ¹H NMR, MS, IR) and thermal studies, a distorted octahedral or square planar {Pd(II) complex} geometry may be proposed for these complexes, the ligand ligates as neutral tetra-, bi- or pentadentate one. All the synthesized compounds were potent anticancer agents. The antibacterial studies of the prepared compounds screened against pathogenic bacteria proved that these compounds exhibit remarkable antibacterial activity.

References

- Prakash, N.B.: Synthesis and studies of tetraaza macrocyclic complexes of transition metal ions. *J. Phys. Appl. Chem.* **1**(2), 17–21 (2014)
- EL-Gammal, O.A., Bekheit, M.M., El-Brashy, S.A.: Synthesis, characterization and in vitro antimicrobial studies of Co(II), Ni(II) and Cu(II) complexes derived from macrocyclic compartmental ligand. *Spectrochim. Acta A* **137**, 207–219 (2015)
- Chandra, S., Kumar, S.: Synthesis and spectral studies on mononuclear complexes of chromium(III) and manganese(II) with 12-membered tetradentate N₂O₂, N₂S₂ and N₄ donor macrocyclic ligands. *Transit. Met. Chem.* **29**, 269–275 (2004)
- Chandra, S., Gupta, R., Gupta, N., Bawa, S.S.: Biologically relevant macrocyclic complexes of copper spectral, magnetic, thermal and antibacterial approach. *Transit. Met. Chem.* **31**, 147–151 (2006)
- Rani, S., Kumar, S., Chandra, S.: Spectroscopic and biological approach in the characterization of a novel 14-membered [N₄] macrocyclic ligand and its Palladium(II), Platinum(II), Ruthenium(III) and Iridium(III) complexes. *Spectrochim. Acta A* **118**, 244–250 (2014)
- Yernale, N.G., Mathada, M.B.H.: Synthesis, characterization, antimicrobial, DNA cleavage, and *In Vitro* cytotoxic studies of some Metal complexes of Schiff base ligand derived from thiazole and quinoline moiety. *Bioinorg. Chem.* **2014**, 1–17 (2014)
- Shiekh, R.A., Rahman, I.A., Malik, M.A.: Synthesis, spectral, electrochemical and biological studies of nitrogen donor macrocyclic ligand and its transition metal complexes. *Int. J. Electrochem. Sci.* **7**, 12829–12845 (2012)
- Swamy, S.J., Pola, S.: Spectroscopic studies on Co(II), Ni(II), Cu(II) and Zn(II) complexes with N₄-macrocyclic ligands. *Spectrochim. Acta A* **70**, 929–933 (2008)
- Ghamami, S., Lashgari, A., Ghahremani Gavineh Roudi, R.: Synthesis and characterization of two new hydrazide palladium complexes. *Can. J. Basic Appl. Sci.* **2**(3), 76–80 (2014)
- Chandra, S., Pipil, P.: Spectral studies of transition metal complexes with 25, 26 dioxo1,6,12,17,23,24 hexaazacyclohexacosia 1,5,12,16 tetraene macrocyclic ligand (L). *J. Chem. Pharma. Res.* **5**(5), 99–104 (2013)
- Singh, D.P., Kumar, K., Sharma, C.: Antimicrobial active macrocyclic complexes of Cr(III), Mn(III) and Fe(III) with their spectroscopic approach. *Eur. J. Med. Chem.* **44**, 3299–3304 (2009)
- Wainwright, K.P.: Applications for polyaza macrocycles with nitrogen-attached pendant arms. *Adv. Inorg. Chem.* **52**, 293–334 (2001)
- Swamy, S.J., Veerapratap, B., Nagaraju, D., Suresh, K., Someshwar, P.: Non-template synthesis of 'N₄' di- and tetraamide macrocyclic ligand with variable ring sizes. *Tetrahedron* **59**, 10093–10096 (2003)
- Kedy, S., Almhna, N., Kandil, F.: Synthesis and characterization of new macrocyclic Schiff bases by the reaction of: 1,7-Bis (6-methoxy-2-formylphenyl)-1,7-dioxheptane and their use in solvent extraction of metals. *Arab. J. Chem.* **8**, 93–99 (2015)
- Fernandes, A.S., Cabral, M.F., Costa, J., Castro, M., Michael, R.D., Drew, G.B., Félix, V.: Two macrocyclic pentaaza compounds containing pyridine evaluated as novel chelating agents in copper(II) and nickel(II) overload. *J. Inorg. Biochem.* **105**, 410–419 (2011)

16. El-Boraey, H.A., Serag El-Din, A.A.: Transition metal complexes of a new 15-membered [N₅] penta-azamacrocyclic ligand with their spectral and anticancer studies. *Spectrochim. Acta A* **132**, 663–671 (2014)
17. Chandra, S., Gupta, L.K.: Spectroscopic approach in characterization of chromium(III), manganese(II), iron(III) and copper(II) complexes with a nitrogen donor tetradentate, 14-membered azamacrocyclic ligand. *Spectrochim. Acta A* **61**, 2139–2144 (2005)
18. Timmons, J.C., Hubin, T.J.: Preparations and applications of synthetic linked azamacrocyclic ligands and complexes. *Coord. Chem. Rev.* **254**, 1661–1685 (2010)
19. El-Boraey, H.A., Emam, S.M., Tolan, D.A., El-Nahas, A.M.: Structural studies and anticancer activity of a novel (N₆O₄) macrocyclic ligand and its Cu(II) complexes. *Spectrochim. Acta A* **78**, 360–370 (2011)
20. El-Boraey, H.A.: Coordination behavior of tetraaza [N₄] ligand towards Co(II), Ni(II), Cu(II), Cu(I) and Pd(II) complexes: Synthesis, spectroscopic characterization and anticancer activity. *Spectrochim. Acta A* **97**, 255–262 (2012)
21. Kang, D., Seo, J., Lee, S.Y., Lee, J.Y., Choi, K.S., Lee, S.S.: First dicadmium(II) complex of tripodal amide ligand with one edge-sharing monocapped octahedral geometry. *Inorg. Chem.* **10**, 1425–1428 (2007)
22. Soliman, A., El-Medani, S., Ali, O.: Thermal study of chromium and molybdenum complexes with some nitrogen and nitrogen-oxygen donor ligands. *J. Therm. Anal. Calorim.* **83**(2), 385–392 (2006)
23. Ajlouni, A.M., Taha, Z.A., Al-Hassan, K.A., Abu Anzeh, A.M.: Synthesis, characterization, luminescence properties and antioxidant activity of Ln(III) complexes with a new aryl amide bridging ligand. *J. Lumin.* **132**, 1357–1363 (2012)
24. Tyagi, M., Chandra, S., Akhtar, J., Chand, D.: Macrocyclic Schiff base ligand and its complexes: inhibitory activity against plant-pathogenic fungi. *Spectrochim. Acta A* **118**, 1056–1061 (2014)
25. Abou-Hussein, A.A., Linert, W.: Synthesis, spectroscopic studies and inhibitory activity against bacteria and fungi of acyclic and macrocyclic transition metal complexes containing a triamine coumarine Schiff base ligand. *Spectrochim. Acta A* **141**, 223–232 (2015)
26. Chandra, S., Qanungo, K., Sharma, S.K.: Synthesis, molecular modeling and spectroscopic characterization of nickel(II), copper(II), complexes of new 16-membered mixed-donor macrocyclic Schiff base ligand incorporating a pendant alcohol function. *Spectrochim. Acta A* **79**, 1326–1330 (2011)
27. Chandra, S., Sharma, A.K.: Nickel(II) and copper(II) complexes with Schiff base ligand 2,6-diacetylpyridine bis(carbohydrazone): synthesis and IR, mass, ¹H NMR, electronic and EPR spectral studies. *Spectrochim. Acta A* **72**, 851–857 (2009)
28. Chandra, S., Ruchi, S.: Synthesis, spectroscopic characterization, molecular modeling and antimicrobial activities of Mn(II), Co(II), Ni(II), Cu(II) complexes containing the tetradentate aza Schiff base ligand. *Spectrochim. Acta A* **103**, 338–348 (2013)
29. El-Gammal, H.A., El-Boraey, O.A.: New 15-membered tetraaza (N₄) macrocyclic ligand and its transition metal complexes: Spectral, magnetic, thermal and anticancer activity. *Spectrochim. Acta A* **138**, 553–562 (2015)
30. Skehan, P., Storeng, R., Scudiero, D., Monks, A., Mahon, J.M., Vistica, D., Warren, J.T., Bokesch, H., Kenney, S., Boyd, M.R.: New colorimetric cytotoxicity assay for anticancer-drug screening. *J. Natl. Cancer Inst.* **82**, 1107–1112 (1990)
31. Wikler, M.A., Cockerill, F. R., Bush, K., Dudley, M.N., Eliopoulos, G.M., Hardy, D.J., Hecht, D.W., Ferraro, M.J., Swenson, J.M., Hindler, J.F., Patel, J.B., Powell, M., Turnidge, J.D., Weinstein, M.P., Zimmer, B.L.: Method for dilution antimicrobial susceptibility tests for bacteria that grow aerobically, approved standard-eighth edition. M07-A8 CLSI: 940 West Valley Road, Suite 1400, Wayne, Pennsylvania **29**(2), 1087–1898 (2009) USA; ISBN: 1-56238-689-1
32. Bayoumi, H.A., Alaghaz, A.M.A., Aljahdali, M.S.: Cu(II), Ni(II), Co(II) and Cr(III) Complexes with N₂O₂-Chelating Schiff's base ligand incorporating azo and sulfonamide moieties: spectroscopic, electrochemical behavior and thermal decomposition studies. *Int. J. Electrochem. Sci.* **8**, 9399–9413 (2013)
33. El-Asmy, A.A., Al-Abdeen, A.Z., El-Maaty, W.M., Mostafa, M.M.: Synthesis and spectroscopic studies of 2,5-hexanedione bis(isonicotinylhydrazone) and its first row transition metal complexes. *Spectrochim. Acta A* **75**, 1516–1522 (2010)
34. Chandra, S., Gupta, L.K.: Mass, EPR, IR and electronic spectroscopic studies on newly synthesized macrocyclic ligand and its transition metal complexes. *Spectrochim. Acta A* **62**, 1125–1130 (2005)
35. Masoud, M.S., Khalil, E.A., Hindawy, A.M., Ali, A.E., Mohamed, E.F.: Spectroscopic studies on some azo compounds and their cobalt, copper and nickel complexes. *Spectrochim. Acta A* **60**, 2807–2817 (2004)
36. Mohamed, G.G., Ibrahim, N.A., Attia, H.A.E.: Spectroscopic studies on some azo compounds and their cobalt, copper and nickel complexes. *Spectrochim. Acta A* **72**, 610–615 (2009)
37. Jayaseelan, P., Prasad, S., Vedanayaki, S., Rajavel, R.: Synthesis, characterization, anti-microbial, DNA binding and cleavage studies of Schiff base metal complexes. *Arab. J. Chem.* (2011). doi:10.1016/j.arabjc.2011.07.029
38. Abd El-halim, H.F., Omar, M.M., Mohamed, G.G.: Synthesis, structural, thermal studies and biological activity of a tridentate Schiff base ligand and their transition metal complexes. *Spectrochim. Acta A* **78**, 36–44 (2011)
39. Venkatachalam, G., Ramesh, R.: Ruthenium(III) bis-bidentate Schiff base complexes mediated transfer hydrogenation of imines. *Inorg. Chem. Commun.* **9**, 703–707 (2006)
40. Geeta, B., Shrivankumar, K., Muralidhar Reddy, P., Ravikrishna, E., Sarangapani, M., Krishna Reddy, K., Ravinder, V.: Binuclear cobalt(II), nickel(II), copper(II) and palladium(II) complexes of a new Schiff-base as ligand: Synthesis, structural characterization, and antibacterial activity. *Spectrochim. Acta A* **77**, 911–915 (2010)
41. Gurumoorthy, P., Ravichandran, J., Karthikeyan, N., Palani, P., Kalilur Rahiman, A.: Template synthesis of polyaza macrocyclic copper(II) and nickel(II) complexes: spectral characterization and antimicrobial studies. *Bull. Korean Chem. Soc.* **33**(7), 2279–2286 (2012)
42. Kavitha, N., Anantha Lakshmi, P.V.: Synthesis, characterization and thermogravimetric analysis of Co(II), Ni(II), Cu(II) and Zn(II) complexes supported by ONNO tetradentate Schiff base ligand derived from hydrazino benzoxazine. *J. Saudi Chem. Soc.* (2015). doi:10.1016/j.jscs.2015.01.003
43. Kivelson, D., Neiman, R.: ESR line shapes in glasses of copper complexes. *J. Chem. Phys.* **35**, 149–155 (1961)
44. Hathaway, B.J., Billing, D.E.: The electronic properties and stereochemistry of mononuclear complexes of the copper(II) ion. *Coord. Chem. Rev.* **5**, 143–207 (1970)
45. Arish, D., Sivasankaran Nair, M.: Synthesis, characterization and biological studies of Co(II), Ni(II), Cu(II) and Zn(II) complexes with pyrrol-L-histidinate. *Arab. J. Chem.* **5**, 179–186 (2012)
46. Osman, A.H.: Synthesis and characterization of cobalt(II) and nickel(II) complexes of some Schiff bases derived from 3-hydrazino-6-methyl[1,2,4] triazin-5(4H)one. *Transit. Metal Chem.* **31**, 35–41 (2006)
47. El-Boraey, H.A.: Structural and thermal studies of some aroyl-hydrazone Schiff's base-transition metal complexes. *J. Therm. Anal. Calorim.* **81**, 339–346 (2005)
48. Emam, S.M., El Sayed, I.E., Nassar, N.: Transition metal complexes of neocryptolepine analogues. Part I: synthesis,

- spectroscopic characterization, and in vitro anticancer activity of copper(II) complexes. *Spectrochim. Acta A* **138**, 942–953 (2015)
49. Coats, A.W., Redfern, J.P.: Kinetic parameters from thermogravimetric data. *Nature* **201**, 68–122 (1964)
50. Horowitz, H.H., Metzger, G.: A New analysis of thermogravimetric traces. *J. Anal. Chem.* **35**, 1464–1468 (1963)
51. Sivakumar, P., Parthiban, K.S., Sivakumar, P., Vinoba, M., Renganathan, S.: Optimization of extraction process and kinetics of *sterculia foetida* Seed oil and its process augmentation for biodiesel production. *Ind. Eng. Chem. Res.* **52**, 8992–8998 (2012)
52. Borsato, D., Galvan, D., Pereira, J.L., Orives, J.R., Angilelli, K.G., Coppo, R.L.: Kinetic and thermodynamic parameters of biodiesel oxidation with synthetic antioxidants: simplex centroid mixture design. *J. Braz. Chem. Soc.* **25**(11), 1984–1992 (2014)
53. Shier, W.T.: *Mammalian cell culture on \$5 a day: a laboratory manual of low cost methods.* University of the Philippines, Los Banos (1991)
54. Chandra, S., Gupta, L.K.: Modern spectroscopic techniques in the characterization of Schiff base macrocyclic ligand and its complexes with transition. *Spectrochim. Acta A* **62**, 307–312 (2005)
55. EL-Asmy, A.A., Rakha, T.H., Abdel-Rhman, M.H., Hassanien, M.M., Al-Mola, A.S.: Synthesis, spectral, thermal and biological studies on N-(2,4-dinitro-phenyl)-2-mercaptoacetohydrazide and its metal complexes. *Spectrochim. Acta A* **136**, 1718–1727 (2015)
56. Gaber, M., El-Wakiel, N.A., El-Ghamry, H., Fathalla, S.K.: Ni(II), Pd(II) and Pt(II) complexes of (1H-1,2,4-triazole-3-ylimino)methyl]naphthalene-2-ol. Structural, spectroscopic, biological, cytotoxicity, antioxidant and DNA binding. *Spectrochim. Acta A* **139**, 396–404 (2015)
57. Zafar, H., Kareem, A., Sherwani, A., Mohammad, O., Ansari, M.A., Khan, H.M., Khan, T.A.: Synthesis and characterization of Schiff base octaazamacrocyclic complexes and their biological studies. *J. Photochem. Photobiol., B* **142**, 8–19 (2015)
58. Kavitha, P., Rama Chary, M., Singavarapu, B.V.V.A., Laxma Reddy, K.: Synthesis, characterization, biological activity and DNA cleavage studies of tridentate Schiff bases and their Co(II) complexes. *J. Saudi Chem. Soc.* **20**, 69–80 (2016)
59. Xiao-Yang, Q., Su-Zhi, L., An-Ran, S., Qian-Qian, L., Bin, Z.: Synthesis, crystal structure and cytotoxic activity of a zinc(II) complex of the Schiff base derived from *S*-benzylthiocarbazate. *Chin. J. Struct. Chem.* **31**(4), 555–561 (2012)
60. Tweedy, B.G.: Plant extracts with metal ions as potential antimicrobial agents. *Phytopathology* **55**, 910–914 (1964)
61. Sonmez, M., Metin, C., Berber, I.: Synthesis, spectroscopic and biological studies on the new symmetric Schiff base derived from 2,6-diformyl-4-methylphenol with N-aminopyrimidine. *Eur. J. Med. Chem.* **45**, 1935–1940 (2010)
62. Singh, D.P., Grover, V., Rathi, P., Jainb, K.: Trivalent transition metal complexes derived from carbonylhydrazide and dimedone. *Arab. J. Chem.* (2013). doi:[10.1016/j.arabjc.2013.07.004](https://doi.org/10.1016/j.arabjc.2013.07.004)